JOURNAL OF
Materials
CHEMISTRY

Study of the dissolution behavior of selenium and tellurium in different solvents—a novel route to Se, Te tubular bulk single crystals

Jun Lu, Yi Xie,* Fen Xu and Liying Zhu

Structure Research Laboratory and Laboratory of Nanochemistry and Nanomaterials,
University of Science and Technology of China, Hefei Anhui 230026, P. R. China.
E-mail: yxie@ustc.edu.cn.

Received 20th April 2002, Accepted 24th May 2002
First published as an Advance Article on the web 6th August 2002

The characteristics of selenium in various solvents under solvothermal conditions were investigated in detail and the different dissolution behavior of selenium in the solvents identified. A brown homogeneous solution was obtained in ethylenediamine. This solution is metastable and is a suitable selenium feedstock for the preparation of selenides at room temperature. A nucleophilic mechanism is proposed for the formation of metal selenides. Millimeter-scale selenium crystals were obtained in the other solvents, *i.e.* ethanol, pyridine, benzene, toluene, and carbon tetrachloride (CCl_4). XRD and ED patterns indicate that the crystals grew in orientation. SEM images show that these crystals have a tubular hexagonal prism morphology with tubular sizes of *ca.* 1–1.5 mm in length, 15 μm in diameter and 5 μm in thickness. We also prepared micro-tubular tellurium crystals in ethylenediamine. The growth mechanism of the tubular crystals is discussed.

Introduction

In recent years, there has been considerable interest in semiconductors of nanometer dimensions due to the quantum size effects that they exhibit.[1–3] Semiconducting metal selenides have been widely used as thermoelectric cooling materials,[4] optical filters,[5] optical recording materials,[6] solar cells,[7] superionic materials,[8] and sensor and laser materials.[9] Several methods have been used for the preparation of metal selenides, such as solid-state reactions,[10] chemical bath deposition,[11] phasegas reactions between the element or its compounds and gaseous H_2Se,[12] and pyrolysis of single source precursors.[13,14] Generally, all these reactions require high temperatures ($\sim$500 °C) and the use of highly toxic or sensitive precursors. Parkin *et al.* reported a low temperature route to selenides in liquid ammonia.[15,16] During their experiments, several manipulations had to be carefully carried out at -77 °C in thick-walled glass vessels, and all operations had to be conducted with care and behind a safety screen. Recently, our group reported a room temperature route to nanocrystalline selenides, in which Se, KBH_4 and MCl_n (M = Zn, Cd, Cu, Bi, Sn) were used as the raw materials and ethylenediamine as the medium.[17] Compared with the previous methods, this technique is relatively mild and no complicated equipment or organometallic precursors are needed, but the products contained H_2 and B_2H_6, which increase the danger and toxicity of the reaction process. Thus, a more suitable and less toxic selenium feedstock is needed to allow the preparation of metal selenides under ambient conditions.

In addition to metal selenides, elemental selenium has also been used widely as a semiconductor material. Elemental selenium exhibits a unique combination of interesting and useful properties;[18] for example, a relatively low melting point ($\sim$490 K), a high photoconductivity ($\sim 8 \times 10^4$ S cm^{-1}), and a high reactivity toward a wealth of chemicals that can be exploited to convert selenium into other functional materials, such as ZnSe and CdSe.[19] The photoelectric and semiconductor properties of selenium are also well known. Selenium is used, for example, in rectifiers, solar cells, photographic exposure meters, and xerography.[20] It can also be used in the glass industry to eliminated bubbles and remove undesired tints produced by iron. As has been observed with other indirect gap semiconductors, such as silicon, the availability of selenium nanostructures with low dimensionality should lead to new applications or enhance the performance of currently existing devices as a result of quantum size effects.[21] Crystalline selenium nanowires and nanoparticles have been produced by several methods.[22–24]

Since the discovery of carbon nanotubes in 1991,[25] compounds with interesting morphologies and specific structures, such as nanotubes, nanorods, nanowires, and microtubules, are currently the focus of much attention due to their special properties.[26] These fascinating systems are expected to exhibit remarkable mechanical, electrical, optical, and magnetic properties that are quite different from their corresponding polycrystalline powder materials. Such low dimensionality materials show potential for application in molecular-based electronic devices, *e.g.* optical memory and switching, display and data records. Many methods have been applied to prepare such low dimensionality materials, for example, WS_2,[27] MoS_2,[28] carbon nanotubes,[29–31] carbides,[32] MgO,[33] GaN[34] and Si_3N_4[35] nanorods or nanowires, and gold microtubules.[36]

Recently, more attention has been directed toward the synthesis of large three-dimensional mesoscale (millimeter- to centimeter-scale) objects.[37–41] Three-dimensional structures suggest new interconnect architecture for electronic and optical systems.[42] The existing technologies for making 3D microstructures are limited stereolithography,[43] free-form laser sintering[44] and traditional casting, machining and assembly, which are difficult with a complex or porous structure. Whitesides reported a procedure to organize millimeter-scale objects into regular, three-dimensional arrays ("crystals") with open structures by self assembly.[45] Newly discovered fullerene-like nest polyhedra (NP) and nanotubules have been observed for metal dichalcogenides,[46–48] and micrometer-sized hexagonal, hollow needles of CdSe have been prepared by electrodeposition from molten salts.[49] Very recently, our group has reported a simple hydrothermal route for the synthesis of β-Ag_2Se[50] and

DOI: 10.1039/b204092a

This journal is © The Royal Society of Chemistry 2002

Sb_2S_3[51] tubular crystals with open structures. However, mesoscale crystals of selenium and tellurium with open structures are, to the best of our knowledge, hitherto unknown.

The solvothermal process, which is conducted at low temperature and does not require organometallic or toxic precursors, has been proven to be a powerful route for preparing new materials.[52] Recently, the solvothermal method has been developed as an alternative route for the synthesis of novel materials,[53] such as GaN[54] and InAs[55] nanoparticles, diamond,[56] and SnSe[57] bulk crystals. Such a process has allowed for the synthesis of several kinds of nanocrystalline selenides.[58,59] Li *et al.*[60] reviewed the development in solvothermal synthesis using ethylenediamine as a reaction medium. However, no detailed discussion on the mechanism of these processes is put forward.

In order to seek a more suitable and generally applicable selenium feedstock, we investigated the characteristics of selenium in various solvents under solvothermal conditions in detail and identified the different dissolution behavior of selenium in those solvents. Specifically, under solvothermal conditions, selenium can combine with ethylenediamine and form a brown homogeneous solution, which readily produces selenides when reacted with various metal salts at room temperature. Moreover, we succeeded in developing a novel method for the preparation of micro-tubular selenium and tellurium crystals by using the solubility characteristics of selenium and tellurium in various solvents. To our best knowledge, this is the first report on the preparation of micro-tubular selenium and tellurium crystals.

Experimental

A Study of the solubility of selenium in various solvents under solvothermal conditions

All reagents were of analytical grade or better and used without further purification. 0.2 g of selenium powder were put into a 50 mL Teflon-lined autoclave, which was filled with solvent up to 85% of its total volume. In the experiments, ethanol, benzene, pyridine, ethylenediamine (en), toluene and carbon tetrachloride were selected as the media. The autoclave was sealed and maintained at 180 °C for 12 h, and then cooled to room temperature. Details of the conditions and results of the experiments are listed in Table 1.

B Preparation of micro-tubular selenium and tellurium crystals

The procedure for the preparation of micro-tubular selenium crystals is similar to experiment A. For the preparation of micro-tubular tellurium crystals, a typical procedure is as follows: 0.2 g tellurium powder were put into a stainless steel 50 mL autoclave, which was filled with solvent up to 85% of its total volume. In the experiments, ethanol, benzene, pyridine, and ethylenediamine were selected as the media. The autoclave was sealed and maintained at 200 °C for 12 h, and then cooled to room temperature. The precipitates were filtered off and washed several times with distilled water and absolute ethanol. Rod-like crystals were obtained and these were then were dried in vacuum at 60 °C for 4 h.

Table 1 Reaction conditions and products for the solvothermal treatment of selenium in various solvents for 12 h at 180 °C

Reaction	Solvent	Product
1	Ethanol	Micrometer single crystals
2	Benzene	Micrometer single crystals
3	Pyridine	Micrometer single crystals
4	Toluene	Micrometer single crystals
5	CCl_4	Micrometer single crystals
6	Ethylenediamine	Brown homogeneous solution

C Characterization

The homogeneous Se–en solution was analyzed by infrared and hydrogen NMR spectra. The IR spectra were recorded in the range 4000–350 cm^{-1} with a Nicolet Model 759 Fourier transform infrared spectrometer, using a KBr wafer, and the hydrogen NMR studies were carried out using a General Electric QE 300 (7.05 T) instrument.

The phases and the crystallographic structure of the products were determined by X-ray diffraction (XRD) using a Japan Rigaku D/max-γA X-ray diffractometer with Cu-Kα radiation (λ = 1.54178 Å). The morphology and size of bulk single crystals were observed using scanning electronic microscopy (SEM), which was performed on an X-650 scanning electron microanalyzer.

Results and discussion

1 Study of solubility of selenium in various solvents under solvothermal conditions

Although selenium is generally described as insoluble in handbooks and texts, our experimental results showed that under solvothermal conditions it can dissolve in some solvents, such as ethanol, benzene, toluene, pyridine, carbon tetrachloride and ethylenediamine (en), and we found that selenium single crystals were obtained in all solvents except for ethylenediamine. The growth of these single crystals maybe the result of a dissolution–recrystallization process. The growth mechanism of the selenium single crystals is discussed in greater detail in section 2 below. The above results suggested that the solvothermal process might allow selenium to be dissolved in some solvents. It was notable that mixing selenium and ethylenediamine under solvothermal condition resulted in a brown homogeneous solution rather than selenium single crystals. The solution may prove to be a useful selenium feedstock; without environmental disturbances, such as visible light illumination or the addition of metal salts, the solution was stable as long as for 20 days. However, when illuminated, the solution became unstable and selenium powder precipitated out.

It is well known that ethylenediamine can chelate many metal cations, and even some anions (*e.g.* Se^{2-} and Te^{2-}), to form polynuclear complexes with a simple chain fragment,[61] furthermore, it is reduced under some conditions. Various nucleophilic selenium species have been widely used in organic synthesis and the interaction of selenium and amines has been reported.[62–64] However, there are no reports on the interaction of selenium and ethylenediamine. Taking into account the strongly nucleophilic properties of ethylenediamine, we propose nucleophilic mechanism for the formation of this homogeneous solution; the structure of this system $[Se(en)_x]$ is schematically illustrated in Fig. 1(a). (The value of x in this structure is assumed to be 2, according to general principles. The actual value is the subject of further study.) Under the solvothermal conditions, when the temperature increased, selenium could be partly reduced by ethylenediamine to form selenium anions with two units of formal negative charge, correspondingly, every ethylenediamine molecular would take one unit of formal positive charge. It is possible that just the existence of these formal charges makes this system somewhat unstable. The IR spectrum of the solution showed an absorption band at 366 cm^{-1} that did not appear in the IR spectrum of ethylenediamine, indicating that selenium interacts with ethylenediamine to produce Se–N covalent bonds. The hydrogen NMR spectrum (Fig. 2) of the solution showed some shifts compared with the standard ethylenediamine solution, presumably also as a result of an interaction between selenium and the ethylenediamine nitogen atoms.

Due to the existence of the formal charge, ethylenediamine combined with selenium in this system becomes unstable,

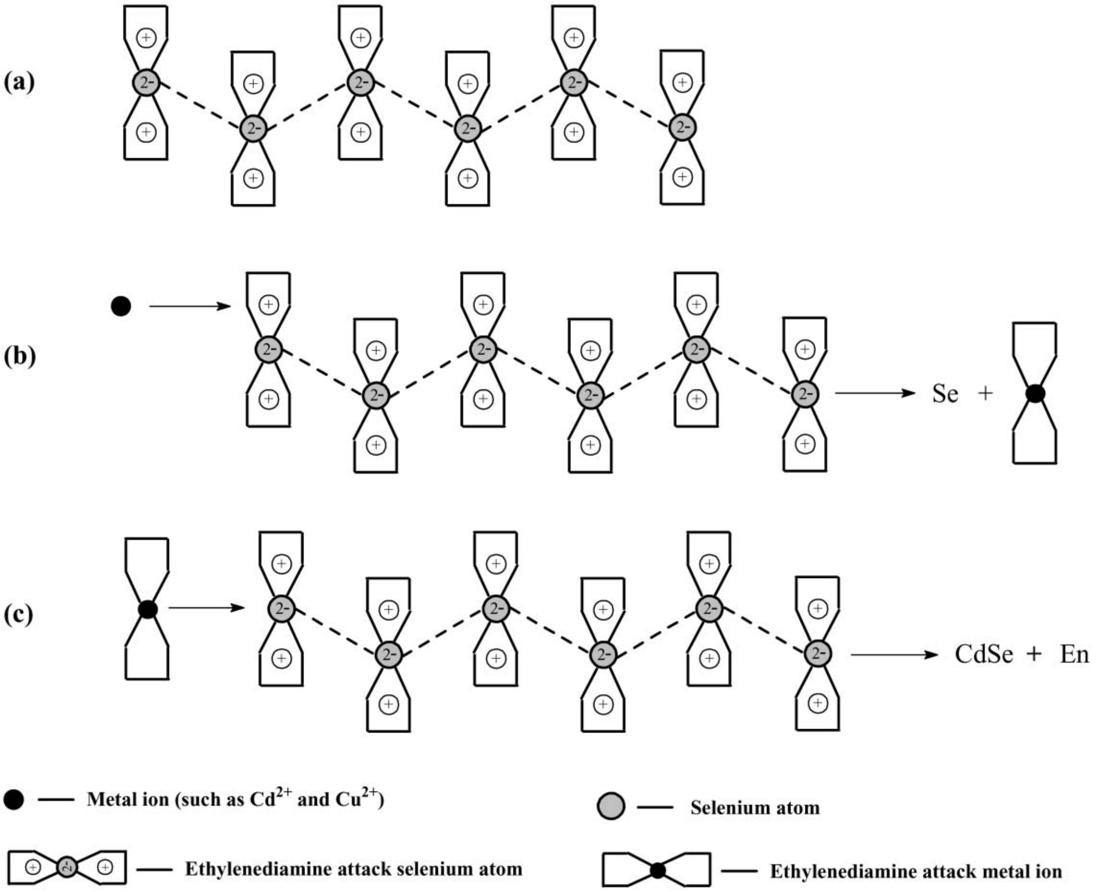

Fig. 1 Schematic illustration of (a) the structure of the Se(en)$_x$ system, (b) the proposed mechanism for direct reaction of metal salts with Se(en)$_x$ and (c) the proposed mechanism for metal salts chelated by en reacting with Se(en)$_x$.

which is thought to be the most sensitive factor affecting the stability of this solution and can be confirmed by the following experiment. When metal salts were added directly to the solution, selenium powder was obtained. This may be because the metal salts initially chelate ethylenediamine that has already combined with selenium [as described in Fig. 1(b)]. In other words, if ethylenediamine in the solution is attacked by other species, the solution becomes relatively unstable, thus, elemental selenium is precipitated. However, when the solution was reacted with metal salts dissolved in ethylenediamine at room temperature, the corresponding selenides were obtained, since elemental selenium in the solution had already been activated by nucleophilic attack of ethylenediamine to form formal Se^{2-} under solvothermal conditions [as described in Fig. 1(c)]. This process is similar to that which occurs when sulfur is activated by amines or hydroxide.[65] The existence of formal Se^{2-} in the solution makes it possible to form metal selenides at room temperature. Thus, this novel solution, Se(en)$_x$, would appear to be a suitable selenium feedstock.

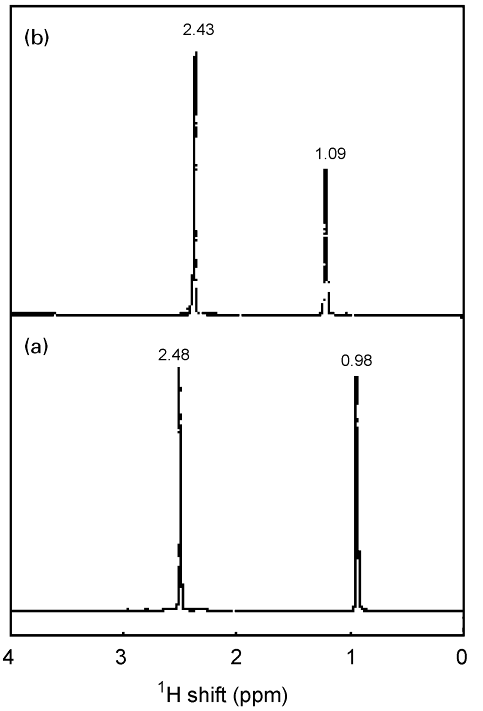

Fig. 2 ^{1}H NMR spectra of (a) Se(en)$_x$ and (b) en.

2 Characterization and growth mechanism of micro-tubular selenium and tellurium crystals

The bulk selenium and tellurium crystals obtained were metallic light grey with a highly reflective lustre. The XRD pattern of polycrystalline selenium powder, prepared by grinding the bulk crystals, is shown in Fig. 3(a). The lattice parameters measured for the sample are a = 4.378 and c = 4.953 Å, which are in good agreement with the reported data for selenium (a = 4.3662 and c = 4.9536 Å),[66] and all the reflection peaks in the pattern can be indexed to the hexagonal selenium phase. The XRD pattern of a single bulk as-prepared selenium crystal [Fig. 3(b)] only exhibits two peaks, at 23.6 and 48.1°, which can be assigned to the 100, and 200 reflections, respectively. Moreover, the other relatively strong reflection peaks in polycrystalline powder diffraction pattern [such as the 101, 102, and 210 reflections in Fig. 1(a)] are absent in this pattern. The above result shows that the (100) face of the selenium crystals runs parallel to the shaft of the bulk single

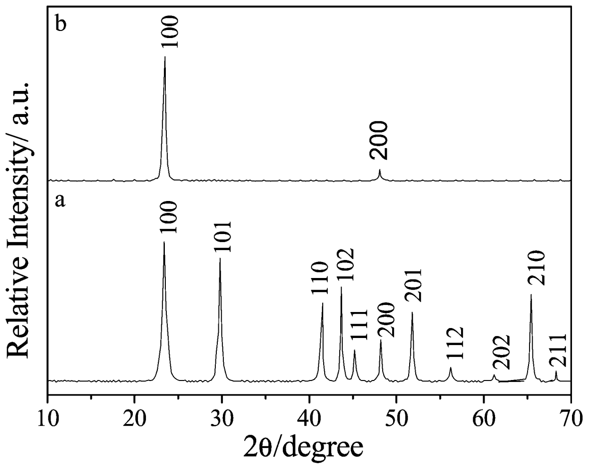

Fig. 3 XRD patterns of (a) powder from ground selenium tubular crystals and (b) a single selenium tubular crystal.

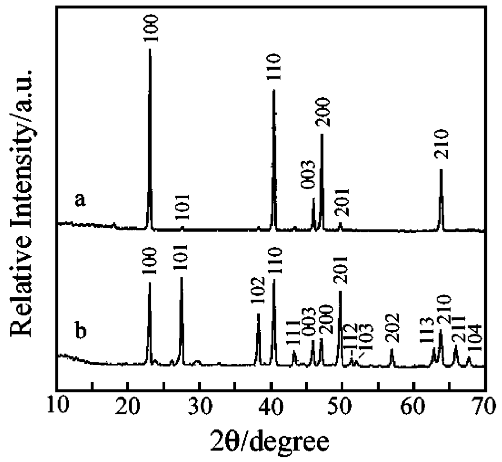

Fig. 4 XRD patterns of (a) powder from ground tellurium tubular crystals and (b) raw tellurium powder.

crystal. Fig. 4(a) shows the XRD pattern of several crushed Te crystals. All the reflection peaks in the pattern can be indexed to the hexagonal tellurium phase, with lattice parameters a = 4.457 and c = 5.919 Å, which are very close to the reported values (a = 4.4496 and c = 5.5914 Å)[67] For comparison, the XRD pattern of the raw tellurium powder is shown in Fig. 4(b). There is a large change in the peak intensity between these two XRD patterns, which is a result of the orientated growth of the tellurium crystals. The XRD pattern of a single needle-like tellurium crystal [Fig 5(a)] only exhibits three peaks, at 23.1, 47.2, and 73.8°, which can be assigned to the 100, 200 and 300 planes, respectively. As for the selenium crystals, the other relatively strong reflection peaks, such as 101, 102, 110, and 201 reflections, in the polycrystalline Te powder diffraction pattern are not present in the pattern of the crushed Te crystals. Fig. 5(b) shows the rocking curve of a single tellurium crystal, which gives an experimental 2θ position of 47.17° for the (200) crystallographic plane ($2\theta_{\mathrm{calc}}$ = 47.2°). It clearly indicates that the (100) face of the tellurium crystals run parallel to the shaft of the bulk single crystal.

It is well known that the most important factor affecting the growth process of single crystals from a solution is the solubility of the solutes. Fig. 6 shows a typical solubility curve showing the temperature–concentration relation; curve AB is called the solubility curve and A′B′ the supersolubility curve, thus, the whole solution region is divided into three parts by these two curves: the stable (S) region, the metastable (M) supersaturation region, and the unstable (U) supersaturation region. From the point of view of single crystal growth, it is desirable that all the solutes released from the solution grow at the surface of the seed crystal rather than other regions of the solution. Thus, among the three regions, the metastable supersaturation region is the most important, due to the fact that the growth process of single crystals takes place in this region. Although selenium and tellurium are generally described as insoluble in handbooks and texts, our experimental results show that under solvothermal conditions they can dissolve in some solvents and then recrystallize. This dissolution and recrystallization process is mainly related to changes in the temperature and pressure of the system. Under solvothermal conditions, when the temperature and pressure of the system increase, selenium or tellurium gradually dissolve in the solvent, then, as the temperature and pressure of the system decrease, the dissolved selenium or tellurium recrystallizes as the single crystals. We can also conclude that the growth process of single crystals takes place in the M region of the solution from the theory discussed above, otherwise no single crystals would be obtained.

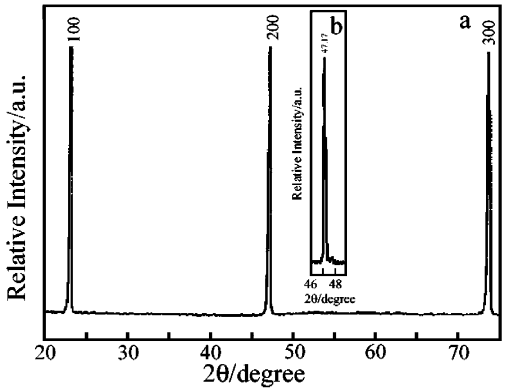

Fig. 5 (a) XRD pattern and (b) the rocking curve of a single tellurium tubular crystal. The rocking curve gives an experimental 2θ position of 47.17° for the (200) crystallographic plane ($2\theta_{\mathrm{calc}}$ = 47.2°).

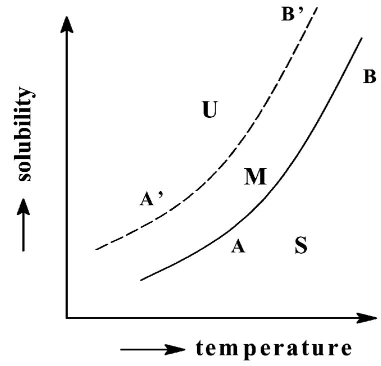

Fig. 6 A typical solubility curve showing the temperature–concentration relation. S, stable region; M, metastable supersaturation region; U, unstable supersaturation region of the solution.

SEM images of the selenium single crystals obtained in various solvents are provided in Fig. 7. They reveal that the crystals obtained in ethanol [Fig. 7(A) and (B)] are tubular hexagonal prisms with uniformity in the lateral dimensions, are straight along their longitudinal axes, and that copious amounts are routinely obtained using this system. Fig. 7(B) gives a magnified view of one of the tubular crystals shown in Fig. 7(A) (marked with an arrow); the crystals have dimensions of *ca.* 1–1.5 mm in length, 15 μm in diameter and 5 μm in

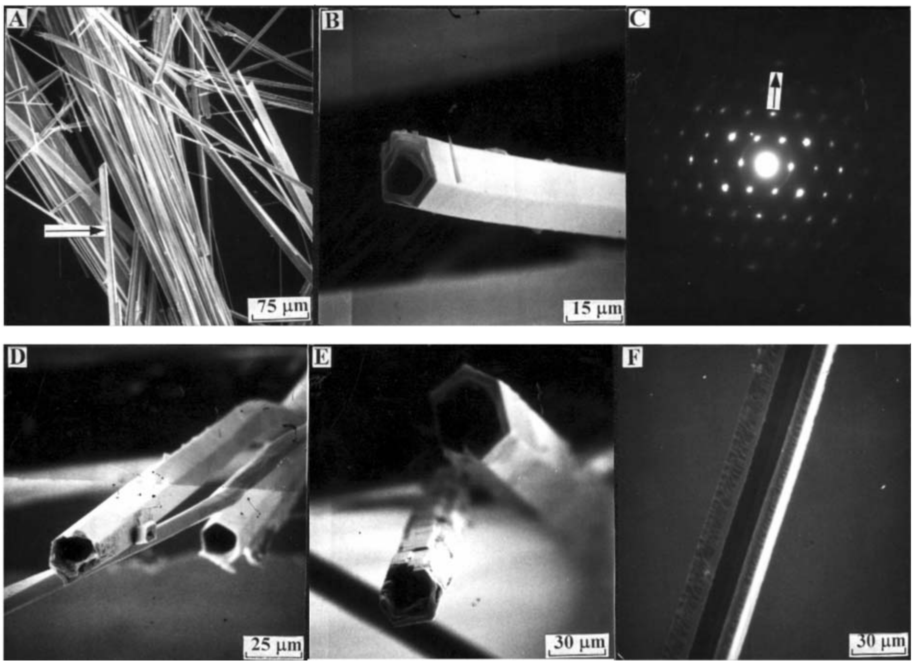

Fig. 7 SEM images of Se bulk crystals obtained from various solvents: (A), (B) ethanol; (D) benzene; (E) carbon tetrachloride; (F) pyridine. (C) ED pattern of selenium crystals obtained from ethanol.

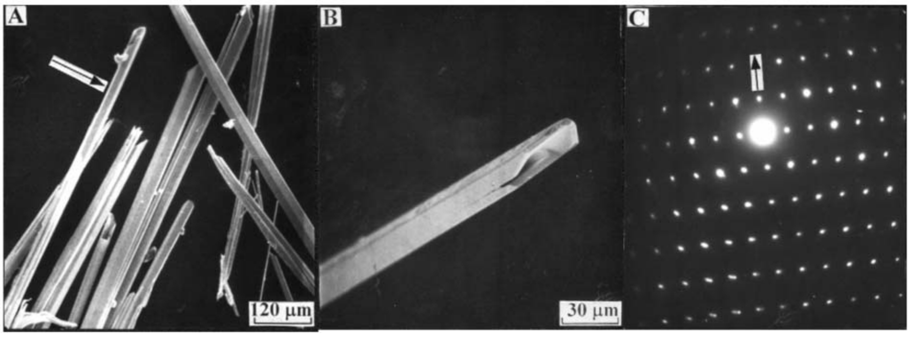

Fig. 8 SEM images and ED pattern of as-grown Te crystals in ethylenediamine.

thickness. The electron diffraction pattern [Fig. 7(C)] of the tubular crystals shows that they grow along the *c* axis. SEM images of the selenium crystals obtained from benzene [Fig 7(D)] and carbon tetrachloride [Fig. 7(E)] confirm that they also show tubular morphology on a similar scale to the crystals obtained in ethanol. It is interesting to note that selenium crystals obtained from pyridine have a semi-closed tubular morphology, which is shown in Fig. 7(F). Fig. 8(A) and (B) show SEM images of as-grown tellurium single crystals obtained from ethylenediamine, from which it can be observed that the tellurium crystals have a tubular hexagonal prism structure; again the electron diffraction pattern suggests that the crystals grow along the *c* axis [Fig. 8(C)]. Typically, these structures are 1–3 mm long, 40–60 μm in diameter and 6–15 μm thick. Unlike the selenium tubular crystals, no tellurium tubular crystal was obtained in other solvents, such as benzene, ethanol, or pyridine. This may be due to the different solubility of selenium and tellurium in solvents under solvothermal conditions.

In order to understand the observed behavior of selenium and tellurium tubular crystals, it is necessary to consider the structure of the trigonal form of the elements. In the following discussion, selenium is used as an example. Selenium is in group VI B of the Periodic Table and has six outer electrons (s^2p^4). Two of these electrons are paired in the s-orbital, two in one of the three p-orbitals, and the remaining two are available for covalent bonding in half-filled p-orbitals. The selenium structure is shown in Fig. 9 and consists of a spiral chain of atoms with three atoms per turn and corresponding atoms in each chain forming a hexagonal network, although the highest symmetry axis is three-fold and is chosen as the *c*-axis. The bonds between atoms on the same chain are covalent, whereas between chains they are thought to be a mixture of electronic and van der Waals.[68] Every selenium atom contacts two atoms

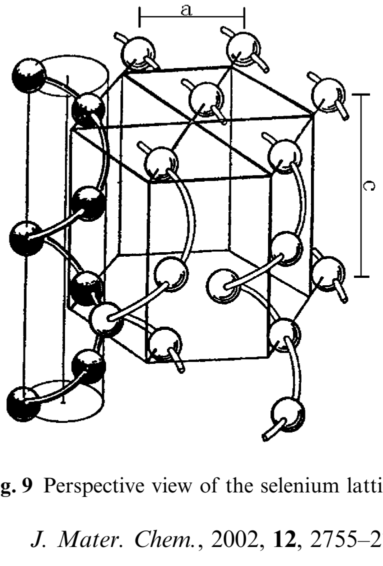

Fig. 9 Perspective view of the selenium lattice.

Fig. 10 SEM image of a single selenium tubular crystal obtained from ethanol, showing an uniform crevice running along the *c* axis.

in the same spiral and four in adjacent spirals, though the former contact is much closer than the latter. This difference is very large and indicates a much greater cohesion between atoms in the same spiral than between those in different spirals. It was suggested by Bradley that this would cause a tendency for crystals to grow in the direction of the trigonal axis more readily than in any other direction. A SEM image (Fig. 10) of one of the tubular selenium crystals shows an uniform crevice running along the *c* axis, which confirms the Bradley's suggestion. Additionally, from the thermodynamic point of view, the surface free energy of the (100) surface is much lower than the corresponding values of the other prismatic surfaces, as shown by the values of the elastic stiffness constants given by Stuck[69] This large difference in surface free energy between the basal and prismatic phase planes results in a strong tendency for the crystals to grow in the form of extended hexagonal prisms, in accordance with the theory of Gibbs[70] that the shape assumed by a growing crystal is that which has minimum surface free energy. Wulff[71] also showed that the equilibrium shape is related to the free energy of the face, and suggested that the crystal faces would grow at rates proportional to their respective surface energies.

The selection of suitable solvents is crucial to the growth of the tubular crystals, especially to the growth of tubular tellurium crystals. In the case of selenium, when ethylenediamine was selected as the medium, only a homogeneous solution rather than tubular crystals was obtained, which shows that the solubility of selenium is obviously greater in ethylenediamine than in other solvents such as ethanol, benzene, and pyridine under solvothermal condition. Tubular tellurium crystals were only obtained in ethylenediamine with our experimental process, which is obviously different from the case for selenium. In other solvents, such as benzene and ethanol, the solubility of tellurium is much lower than that of selenium, which may result in a narrowing of the M region of the solution. Thus, it is possible to severly limit the recrystallizing process, the process by the tubular tellurium crystals are formed.

Conclusion

The dissolution behavior of selenium and tellurium in different solvents has been investigated. Under solvothermal condition, selenium dissolved in solvents such as ethanol and ethylenediamine. A brown homogeneous solution was obtained in ethylenediamine, and was found to be a suitable selenium feedstock for the preparation of selenides at room temperature. The growth of millmeter-scale tubular Se and Te crystals by a recrystallization process of selenium and tellurium powders in different solvents is reported for the first time. SEM images show that the tubular selenium crystals are *ca.* 1–1.5 mm long, 15 μm in diameter, and 5 μm thick, and the tellurium examples are 1–3 mm long, 40–60 μm in diameter, and 6–15 μm thick. The selection of the solvents is critical for the growth of the tubular crystals, especially in the case of tellurium. The growth of the tubular crystals occured *via* a dissolution–recrystallization process.

Acknowledgement

Financial support from the Chinese National Foundation of Natural Science Research is gratefully acknowledged.

References

1 S. Gorer and G. Hodes, *J. Phys. Chem. B*, 1994, **98**, 5338.
2 B. Ludolph, M. A. Malik, P. O'Brein and N. J. Revaprasadu, *Chem. Commun.*, 1998, 1849.
3 S. A. Empedocls and M. G. Bawendi, *J. Phys. Chem. B*, 1999, **103**, 1826.
4 T. C. Harman, *WO Pat. Appl.*, 9 416 465, 1994; *US Pat. Appl.*, 2 451 12, 1994.
5 T. Hayshi and Y. Hiroshi, *Jpn. Kokai Tokkyo Koho*, JP 02 1995, **173**, 622.
6 F. Mongellaz, A. Fillot, R. Griot and J. De Lallee, *Proc. SPIE-Int. Soc. Opt. Eng.*, 1994, **156**, 2227.
7 S. T. Lakshmikvmar, *Sol. Energy Mater. Sol. Cells*, 1994, **32**, 7.
8 A. A. Korzhuev, *Fiz. Khim. Obrab.-Mater.*, 1991, **3**, 131.
9 D. A. Kondas, *Report*, ARFSD-TR-92024, Order No. ADA260781, Blackwell Science, Oxford, 1993, 26 pp.
10 R. J. Coustal, *J. Chim. Phys.*, 1958, **38**, 277.
11 C. D. Lokhnade, P. S. Patil, H. Tributsch and A. Ennaoui, *Sol. Energy Mater. Sol. Cells*, 1998, **55**, 379.
12 H. C. Metcalf, J. E. Williams and J. F. Caskta, *Modern Chemistry*, Holt Reinhart Winston, New York, 1982, p. 54.
13 M. L. Steigerwald, A. P. Alivisatos and J. M. Gibson, *J. Am. Chem. Soc.*, 1988, **110**, 3046.
14 V. Ptatschek, B. Schreder and K. Hertz, *J. Phys. Chem. B*, 1997, **101**, 8898.
15 G. Henshaw, I. P. Parkin and G. Shaw, *Chem. Commun.*, 1996, 1095.
16 G. Henshaw, I. P. Parkin and G. Shaw, *J. Chem. Soc., Dalton Trans.*, **1997**, 231.
17 W. Wang, Y. Geng, P. Yan, F. Liu, Y. Xie and Y. Qian, *J. Am. Chem. Soc.*, 1999, **121**, 4062.
18 L. I. Berger, *Semiconductor Materials*; CRC Press, Boca Raton, FL, 1997, pp. 86–88.
19 E. Best, I. Hinz and H. Wendt, in *Gmelin Handbuch der Anorganische Chemie*, ed. H. Karl Kugler, Spring-Verlag, Berlin, 1979, vol. 10. pp. 168–180.
20 J. A. Johnson, L. M. Saboungi and D. J. Meisel, *J. Phys. Chem. B*, 1999, **103**, 59.
21 M. J. Sailor and K. L. Kavanagh, *Adv. Mater.*, 1992, **4**, 432.
22 G. Khitrov, *MRS Bull.*, 2000, **25**, 5.
23 A. Abdelouas, W. L. Gong, W. Lutze, J. A. Shelnutt, R. Franco and I. Moura, *Chem. Mater.*, 2000, **122**, 1510.
24 B. Gates, Y. Yin and Y. Xia, *J. Am. Chem. Soc.*, 2000, **122**, 12582.
25 S. Iijima, *Nature*, 1991, **354**, 56.
26 A. M. Rao, E. Rithter, S. Bandow, B. Chase, P. C. Eklund, K. A. Williams, S. Fang, K. R. Subbaswamy, M. Menon, A. Thess, R. E. Smalley, G. Dresselhaus and M. S. Dresselhaus, *Science*, 1997, **275**, 187.
27 R. Tenne, L. Margulis, M. Genut and G. Hodes, *Nature*, 1992, **360**, 444.
28 Y. Feldman, E. Wasserman, D. J. Srolovitz and R. Tenne, *Science*, 1995, **267**, 222.
29 N. G. Chopra, R. J. Luyken, K. Cherrey, V. H. Crespi, M. L. Cohen, S. G. Souie and A. Zettl, *Science*, 1995, **269**, 966.
30 Z. Weng-Sieh, K. Cherrey, N. G. Chopra, X. Blase, Y. Miyamoto, A. Rubio, M. L. Cohen, S. G. Louie, A. Zettl and R. Gronsky, *Phys. Rev. B*, 1995, **51**, 11229.
31 D. D. Archibald and S. Mann, *Nature*, 1991, **363**, 430.
32 H. Dai, E. W. Wong, Y. Z. Lu, S. S. Fan and C. M. Lieber, *Nature*, 1995, **375**, 769.
33 P. D. Yang and C. M. Lieber, *Science*, 1996, **273**, 1836.
34 W. Q. Han, S. S. Fan, Q. Q. Li and Y. D. Hu, *Science*, 1997, **277**, 1287.
35 W. Q. Han, S. S. Fan, Q. Q. Li, B. L. Gu, X. B. Zhang and D. P. Yu, *Appl. Phys. Lett.*, 1997, **71**, 2271.
36 W. Liang and C. R. Martin, *J. Am. Chem. Soc.*, 1990, **112**, 9666.
37 J. Tein, T. L. Breen and G. M. Whitesides, *J. Am. Chem. Soc.*, 1998, **120**, 12670.

38 A. Terfort, N. Bowden and G. M. Whitesides, *Nature*, 1997, **386**, 162.
39 H. Lin and C. Mou, *Science*, 1996, **273**, 765.
40 S. Schacht and Q. Huo, *Science*, 1996, **273**, 768.
41 J. Y. Ying and C. P. Mehnert, *Angew. Chem., Int. Ed.*, 1999, **38**, 56.
42 M. Koyanagi, *Proc. SPIE-Int. Soc. Opt. Eng*, 1991, **1390**, 467.
43 J.-J. Clair, *J. Mater. Process. Technol.*, 1996, **57**, 393.
44 F. E. DeAngelis, *Proc. SPIE-Int. Soc. Opt. Eng.*, 1991, **1598**, 61.
45 T. L. Breen, J. Tein, S. R. J. Oliver, T. Hadzic and G. M. Whitesides, *Science*, 1999, **284**, 948.
46 K. Chihiro, S. Yoshio and S. Kazuo, *J .Cryst. Growth.*, 1989, **94**, 967.
47 R. Tenne, L. Margulis, M. Genut and G. Hodes, *Nature.*, 1992, **360**, 444.
48 M. Hershfinkel, L. A. Gheber, V. Volterra, J. L. Hutchison, L. Margulis and R. Tenne, *J. Am. Chem. Soc.*, 1994, **116**, 1914.
49 H. Minoura, T. Negoro, M. Kitakata and Y. Ueno, *Sol. Energy Mater.*, 1985, **12**, 335.
50 J. Hu, B. Deng, Q. Lu, K. Tang, R. Jiang, Y. Qian, G. Zhou and A. Cheng, *Chem. Commun.*, 2000, 715.
51 Q. Yang, K. Tang, C. Wang, Y. Qian, W. Yu, G. Zhou and F. Li, *J. Mater. Chem.*, 2001, **11**, 257.
52 G. J. Demazeau, *J. Mater. Chem.*, 1999, **9**, 15.
53 W. S. Sheldrick and M. Wachhold, *Angew. Chem., Int. Ed. Engl.*, 1997, **36**, 206 and references therein.
54 Y. Xie, Y. Qian, W. Wang, S. Zhang and Y. Zhang, *Science*, 1996, **272**, 1926.
55 Y. Li, X. Duan, Y. Qian, L. Yang, M. Ji and C. Li, *J. Am. Chem. Soc.*, 1997, **119**, 7869.
56 Y. Li, Y. Qian, H. Liao, Y. Ding, L. Yang, C. Xu, F. Li and G. Zhou, *Science*, 1998, **281**, 246.
57 B. Li, Y. Xie, J. Huang and Y. Qian, *Inorg. Chem.*, 2000, **39**, 2061.
58 Y. Li, Y. Ding, Y. Qian, Y. Zhang and L. Yang, *Inorg. Chem.*, 1998, **37**, 2844.
59 Y. Li, Y. Ding, Y. Qian, Y. Zhang and L. Yang, *Inorg. Chem.*, 1998, **38**, 1382.
60 J. Li, Z. Chen, R. J. Wang and D. M. Proserpio, *Coord. Chem. Rev.*, 1999, **192**, 707.
61 J. D. Corbett, *Chem. Rev.*, 1985, **85**, 383.
62 G. Mugesh, A. Panda, H. B. Singh and R. J. Butcher, *Chem.-Eur. J.*, 1999, **5**, 1411.
63 M. Iwaoka and S. Tomoda, *Organoselenium Chem.*, 2000, **208**, 55.
64 P. Renaud, *Organoselenium Chem.*, 2000, **208**, 81.
65 T. Jiang, G. A. Ozin and R. L. Bedard, *Adv. Mater.*, 1994, **6**, 860.
66 Joint Committee on Powder Diffraction Standards (JCPDS), File No. 6-362.
67 Joint Committee on Powder Diffraction Standards (JCPDS), File No. 36-1452.
68 A. V. Hippel, *J. Chem. Phys.*, 1948, **16**, 372.
69 J. Stuck, *The Physics of Selenium and Tellurium*, ed. W. C. Cooper, Pergamon, Oxford, 1969.
70 J. W. Gibbs, *Scientific Paper*, vol. 1, 1906.
71 G. Z. Wulff, *Krist.*, 1901, **34**, 449.